Asia Pac. J. Math. 2026 **13**:104

A NETWORK-BASED COMPARTMENTAL MODELING FRAMEWORK FOR ENVIRONMENTALLY MEDIATED FASCIOLIASIS TRANSMISSION

HADIJA PHILIPO1*, ALFRED HUGO, MONICA KUNG'ARO, JAIROS SHINZEH

Department of Mathematics and Statistics, University of Dodoma, Box 338,

Dodoma, Tanzania

*Corresponding author: hadijaphilipo63@gmail.com

Received Jan. 19, 2026

Abstract. Fascioliasis remains a parasitic disease of substantial veterinary importance, driven by coupled transmission processes involving cattle, freshwater snails, and contaminated environments. Many existing compartmental models assume homogeneous mixing, an assumption that may poorly reflect the spatially clustered and occasionally long-range contacts characteristic of smallholder livestock networks. In this study, we develop and analyze a network-based compartmental framework that embeds multihost fascioliasis dynamics within a small-world contact structure representing interactions among farm villages. The model explicitly incorporates cattle, snail, and environmental compartments and distinguishes between frequent local transmission and rare long-distance cattle movements introduced through network rewiring. Analytical results are used to derive the basic reproduction number and characterize the disease-free equilibrium, while numerical simulations are employed to investigate how network connectivity influences infection persistence. Sensitivity analysis highlights environmental contamination, snail-related parameters, and local contact intensity as the dominant contributors to transmission dynamics. Simulation-based control scenarios further indicate that interventions targeting environmental contamination and local transmission pathways produce greater reductions in infection prevalence than strategies focused solely on restricting long-distance cattle movement. These findings underscore the importance of accounting for heterogeneous contact structures when modeling fascioliasis transmission. The proposed network-based framework offers a flexible methodological approach that can be adapted to other environmentally mediated parasitic diseases.

2020 Mathematics Subject Classification. 92D30.

Key words and phrases. Fascioliasis; network based modeling; environmental transmission; small world networks; computational epidemiology; multihost networks.

1. Introduction

Fascioliasis is a neglected zoonotic parasitic disease with a wide geographical distribution across tropical and subtropical regions, where grazing practices frequently expose cattle to contaminated

DOI: 10.28924/APJM/13-104

water and vegetation [1]. The disease is caused by trematodes of the genus *Fasciola*, primarily *Fasciola hepatica* and *Fasciola gigantica*, which infect domestic ruminants including cattle, sheep, and goats [2]. Transmission is sustained through freshwater snails of the family Lymnaeidae, which act as obligatory intermediate hosts and support parasite development from miracidia to cercariae [3]. Eggs shed in the feces of infected cattle hatch into miracidia that penetrate snail tissues, undergo asexual development, and eventually produce cercariae that encyst as metacercariae on aquatic vegetation or water surfaces, forming the infective stage for mammalian hosts.

Cattle acquire infection primarily through grazing on contaminated pastures or drinking from water sources containing metacercariae. Following ingestion, metacercariae excyst in the intestine and migrate through the liver parenchyma, causing mechanical damage and inflammatory responses [4]. Adult flukes subsequently establish in the bile ducts, where they feed on blood and bile, leading to pathological outcomes such as hepatic fibrosis, biliary obstruction, weight loss, reduced milk yield, impaired fertility, and increased susceptibility to secondary infections [1]. These effects collectively reduce animal productivity and compromise herd health, particularly in extensive and semi-intensive cattle production systems.

Fascioliasis is estimated to affect more than 600 million livestock animals globally [5], with documented cases across Europe, the Americas, Asia, Oceania, and Africa [6]. In Africa, high prevalence rates have been reported in countries such as Nigeria, Ethiopia, Zambia, and Uganda [7]. In Tanzania, fascioliasis is endemic but remains underreported in routine surveillance. Available studies indicate prevalence levels ranging from 47.6% to 63.8% in traditional cattle production systems [8], while retrospective abattoir surveys report infection rates of approximately 70% in Morogoro and 52.6% in Arusha [9]. These findings highlight sustained transmission in local cattle populations.

Beyond its epidemiological significance, fascioliasis imposes substantial economic losses on cattle production networks [10,11]. These losses arise from liver condemnation at slaughter, reduced growth rates, decreased milk production, reproductive impairment, and increased veterinary costs [12]. Globally, fascioliasis in cattle is estimated to cause economic losses of approximately USD 3 billion annually [13]. In Tanzania, abattoir based assessments have reported annual financial losses of around USD 280 at the Arusha abattoir alone due to condemnation of infected livers [14]. Despite this burden, effective control remains challenging because transmission depends on coupled interactions among environmental contamination, snail populations, and heterogeneous cattle movements.

Mathematical modeling provides a useful framework for investigating these coupled transmission mechanisms and for evaluating potential control strategies. Most existing fascioliasis models employ classical compartmental formulations, such as SIR or SEIR structures, and typically assume homogeneous mixing within host populations [15]. In practice, cattle contacts are shaped by herd organization,

grazing routes, shared water points, and occasional long distance movements between farming communities. These features introduce spatial clustering and heterogeneity that are not adequately captured by homogeneous mixing assumptions.

Network-based epidemiological models offer a natural extension by explicitly representing heterogeneous contact patterns and identifying structural features that influence disease spread [16]. Such approaches have been successfully applied to livestock and wildlife diseases, including bovine tuberculosis and foot-and-mouth disease, where network structure strongly affects outbreak size and persistence [17,18]. However, network-based modeling remains relatively underexplored in the context of fascioliasis, particularly for systems that involve environmentally mediated transmission, spatially localized snail habitats, and intermittent cattle movement between farm villages [19].

In this study, we develop a network-based compartmental modeling framework that integrates multihost fascioliasis dynamics with a small-world network architecture representing interactions among farm villages. The framework captures both frequent local transmission driven by shared environments and rare long distance connections arising from cattle movements. By combining cattle, snail, and environmental compartments within a structured contact network, the model enables a systematic investigation of how clustering, long range links, and environmental contamination influence disease persistence and control effectiveness. The proposed approach contributes a flexible and reproducible modeling framework that can be extended to other environmentally transmitted parasitic diseases characterized by heterogeneous contact structures.

2. Model Formulation

This section formulates an intra–farm village model that captures fascioliasis transmission within individual farm villages embedded in a farm–village network. The model integrates a small–world contact structure to represent both frequent local interactions and occasional long distance connections.

Smallholder cattle networks typically involve intensive local interactions—such as communal grazing and shared water sources—while long distance movements occur irregularly through trade, seasonal transhumance, or flooding. These characteristics are well captured by small–world networks, which combine high local clustering with a small average path length [20]. This topology is therefore more suitable than scale–free networks, which require hub like structures that are uncommon in smallholder livestock networks [21]. In a small–world network, disease transmission depends strongly on the clustering coefficient: high clustering intensifies local transmission, whereas increased longrange links reduce local saturation and enable rapid spread across distant communities [22].

2.1. **Model Description.**

The model integrates a classical fascioliasis compartmental structure with a small–world network representation. Each farm village is treated as a node, and the model tracks the dynamics of cattle, snails, and environmental contamination within each node. Transmission

between nodes occurs through local contacts with probability p_s and rare long distance interactions with probability p_l.

Susceptible cattle $S_c(t)$ become exposed $L_c(t)$ after ingesting metacercariae from contaminated vegetation or water. Exposed cattle progress to the infectious class $I_c(t)$, where they shed eggs into the environment. Infectious cattle may recover with temporary immunity $R_c(t)$ or die due to disease at rate ρ. Immunity wanes at rate θ, returning individuals to the susceptible pool.

In the network interpretation, cattle labeled by x represent individuals exposed to metacercariae through local environment with probability p_s, while cattle labeled by y represent those exposed through long distance contacts with probability p_l. Each contaminated environment can infect its k nearest neighbor cattle with probability p_s, while rare long distance links provide infection risk with probability p_l.

Susceptible snails $S_n(t)$ become infected after miracidia penetrate their tissues. After a latent period $L_n(t)$, snails progress to the infectious class $I_n(t)$ and release cercariae that encyst as metacercariae. The environmental reservoir $M(t)$ represents the density of metacercariae in water and vegetation. Metacercariae accumulate from infectious snails at rate η and from eggs shed by infectious cattle at rate α. Environmental contamination decays at rate δ.

Therefore, the complete model is, therefore, described by a system of ordinary differential equations:

$$\begin{cases} \dfrac{dS_c}{dt} = \pi_c + \theta R_c - \lambda_c S_c - \mu_c S_c, \\ \dfrac{dL_c}{dt} = \lambda_c S_c - \gamma_c L_c - \mu_c L_c, \\ \dfrac{dI_c}{dt} = \gamma_c L_c - (\omega + \mu_c + \rho) I_c, \\ \dfrac{dR_c}{dt} = \omega I_c - \theta R_c - \mu_c R_c, \\ \dfrac{dS_n}{dt} = \pi_n - \lambda_n S_n - \mu_n S_n, \\ \dfrac{dL_n}{dt} = \lambda_n S_n - \gamma_n L_n - \mu_n L_n, \\ \dfrac{dI_n}{dt} = \gamma_n L_n - \mu_n I_n, \\ \dfrac{dM}{dt} = \eta I_n + \alpha I_c - \delta M. \end{cases} \tag{1}$$

with initial conditions (ICs) given by

$$S_c(0) > 0, \quad L_c(0) \geq 0, \quad I_c(0) \geq 0, \quad R_c(0) \geq 0, \quad S_n(0) > 0, \quad L_n(0) \geq 0, \quad I_n(0) \geq 0, \quad M(0) \geq 0.$$

where λ_c and λ_n represent the forces of infection given by;

$$\lambda_c(t) = \left(P_s k x + P_l y\right) M(t), \quad \lambda_n(t) = P_n\, I_c(t)$$

The combination of parameters $P_s kx + P_l y$ denotes the coefficient of cattle effective exposure from metacercariae and p_n represents coefficient of snail effective exposure from infectious cattle (captures miracidia production and the probability of infection). The model is built under a number of explicit assumptions, listed here to clarify the scope and limitations:

i. Egg deposition, egg development and miracidia dynamics are not modeled explicitly; instead snail infection is approximated as proportional to I_c. This reduces complexity but collapses time delays and environmental factors (temperature, desiccation) that govern egg hatching and miracidia survival.

ii. All cercariae derived metacercariae are grouped into a single environmental compartment M, with linear input from infectious snails (ηI_n) and exponential decay (δM), a common simplification in fascioliasis models when substrate specific deposition and climate dependent survival data are limited [23].

iii. Birth or recruitment and natural mortality rates are constant in time; seasonal or density dependent snail demography and density regulation for snail populations are not included here.

iv. The baseline formulation does not include an additional disease induced mortality term for infectious snails.

v. Humans contribution of fasciola parasites on environment is neglected.

Table 1. Description of model variables.

Variable	**Description**
S_c	Susceptible cattle population
L_c	Exposed (latent) cattle infectious but the symptoms are not yet seen
I_c	infectious cattle shedding eggs into the environment
R_c	Recovered cattle with temporary immunity
S_n	Susceptible snail population
L_n	Exposed (latent) snails infectious but symptoms are not yet seen
I_n	infectious snails releasing cercariae into water
M	Density of metacercariae in the environment

TABLE 2. Descriptions of model Parameters.

Parameter	Description	Value	Sources
π_c	Recruitment rate of cattle	10 cattle/day	[24]
θ	Loss of immunity rate in recovered cattle	0.01 day^{-1}	[25]
γ_c	Progression rate from latent to infectious cattle	0.20 day^{-1}	[26]
ω_c	Recovery rate of infectious cattle	0.10 day^{-1}	[27]
μ_c	Natural mortality rate of cattle	0.01 day^{-1}	[28]
ρ_c	Disease induced mortality of cattle	0.01 day^{-1}	[29]
p_s	Probability of short-range transmission	0.25	[30]
p_l	Probability of long-range transmission	0.15	[30]
k	Average number of local contacts per cattle	0.02 contacts/day	Assumed
x	Proportion of infectious individuals in local contacts	0.4	[31]
y	Proportion of infectious individuals from far environment	0.6	[32,33]
π_n	Recruitment rate of snails	100 snails/day	[34]
p_n	Transmission coefficient from infectious cattle to susceptible snails	0.12 day^{-1}	[35]
γ_n	Progression rate from latent to infectious snails	0.30 day^{-1}	[36]
μ_n	Natural mortality rate of snails	0.10 day^{-1}	[37]
η	Shedding rate of metacercariae from infectious snails	0.10/day	[38]
α	Contribution of infectious cattle to environmental contamination	0.05/day	[39,40]
δ	Natural decay rate of metacercariae in environment	0.20 day^{-1}	[41]

From model system (1), Figure 1, Table 1 and Table 2 were obtained.

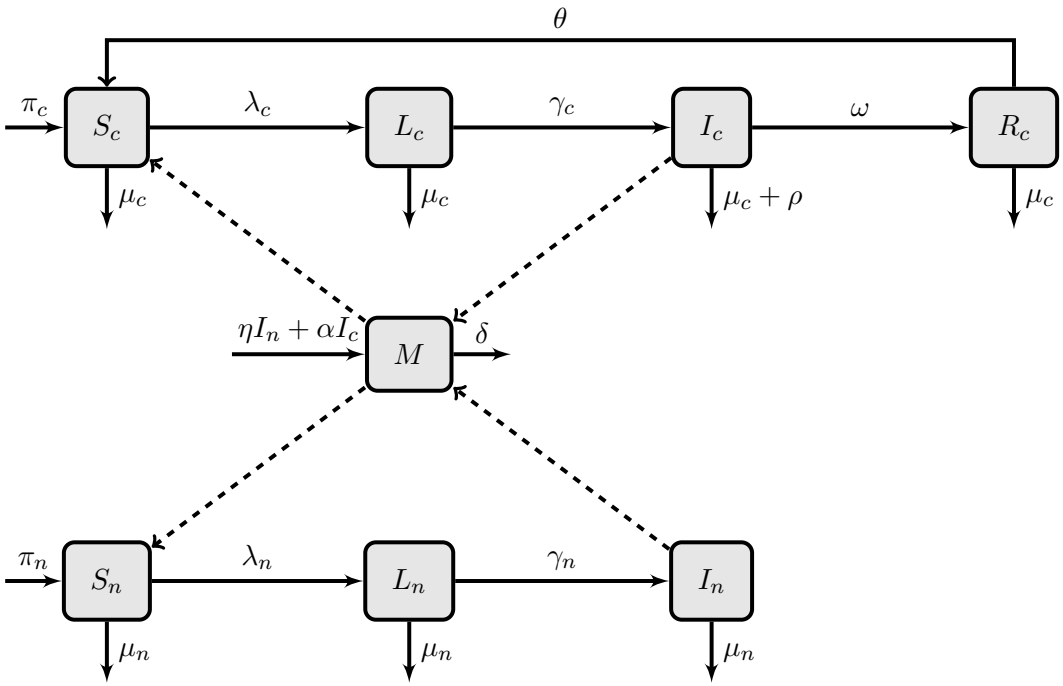

FIGURE 1. Flow diagram of the Fascioliasis transmission model.

2.2. **Complex Network Structure and Model Biological Clarifications.** The contact structure among cattle populations across farm villages is modeled using a small world network framework, following the formulation of Watts and Strogatz [42]. Each node in the network represents a cattle subpopulation within a farm village, while edges represent potential transmission pathways mediated through shared grazing areas, watering points, or environmental contamination.

The network is initially constructed as a regular ring lattice of N nodes, where each node is connected to its k nearest neighbors, representing frequent short range interactions within geographically proximate farm villages. These local connections capture biologically realistic processes such as communal grazing and shared water sources, which facilitate repeated exposure to infective metacercariae.

To account for occasional long distance cattle movements due to trade, transhumance, flooding, or seasonal pasture sharing, each local edge is rewired with probability p_l to a randomly chosen node in the network. This rewiring process introduces long range links while preserving a high clustering coefficient, a defining property of small world networks. The resulting network therefore exhibits strong local clustering combined with a small average path length, consistent with observed livestock movement patterns in smallholder farming systems [43].

Mathematically, the probability of a connection between node i and node j is given by

$$P_{ij} = \begin{cases} p_s, & \text{if } j \in \mathcal{N}_k(i), \\ jp_l, & \text{if } j \notin \mathcal{N}_k(i), \end{cases}$$

where $\mathcal{N}_k(i)$ denotes the set of k nearest neighbors of node i, p_s is the short range transmission probability, and p_l is the long range transmission probability with $p_l \ll p_s$.

Several network metrics are relevant for disease transmission dynamics. The clustering coefficient quantifies the likelihood that neighboring farm villages are also connected, thereby amplifying localized transmission. Betweenness centrality identifies nodes that lie on many shortest paths, corresponding to farm villages that act as transmission bridges between otherwise weakly connected clusters. Modularity reflects the presence of subgroups within the network, which may correspond to geographically or socially distinct farming communities.

In this study, the small-world topology and associated parameters (k, p_s, and p_l) are treated as biologically motivated assumptions based on livestock management practices reported in the literature. The epidemiological consequences of these network features such as their effects on infection persistence, outbreak size, and control effectiveness are subsequently validated through numerical simulations and sensitivity analysis.

3. Numerical Analysis of the Model

This section describe the computations that transform theoretical equations into practical equations and interpret how diseases spread, persist, and can be controlled. The model used in this study is described by a nonlinear system (1) of differential equations. Analysis is very important because these equations often cannot be solved analytically owing to nonlinear terms.

3.1. **Basic properties of the model.**

Model properties are foundational concepts in epidemiological modeling. It is clear that, epidemiological models must satisfy essential properties such as positivity, boundedness, and the existence of an invariant region to ensure biological realism and mathematical validity [44]. These properties guarantee that the population compartments (susceptible, latent and infectious) remain non negative and confined within feasible limits over time.

3.1.1. *Positivity of Solutions.*

Since model system (1) describes the populations of cattle, snails, and environmental metacercariae, it is important to show that all state variables remain non negative for all times $t \geq 0$.

Lemma 1. *Suppose that initial conditions satisfy*

$$\big(S_c(0), L_c(0), I_c(0), R_c(0), S_n(0), L_n(0), I_n(0), M(0)\big) \in \mathbb{R}^8_+.$$

Then the solution

$$\big(S_c(t), L_c(t), I_c(t), R_c(t), S_n(t), L_n(t), I_n(t), M(t)\big)$$

of the system (1) remains non negative for all $t \geq 0$.

Proof. Consider the first equation of system (1):

$$\frac{dS_c}{dt} = \pi_c + \theta R_c - \lambda_c S_c - \mu_c S_c \geq -(\lambda_c + \mu_c) S_c. \tag{2}$$

Integrating both sides and using the initial condition $S_c(0) \geq 0$ gives

$$S_c(t) \geq S_c(0)\, \exp\left(-\int_0^t (\lambda_c + \mu_c)\, ds\right) \geq 0. \tag{3}$$

Applying the same argument to the remaining equations yields

$$L_c(t) \geq L_c(0) \exp\big[-(\gamma_c + \mu_c)t\big] \geq 0 \tag{4}$$

$$I_c(t) \geq I_c(0) \exp\big[-(\omega + \mu_c + \rho)t\big] \geq 0 \tag{5}$$

$$R_c(t) \geq R_c(0) \exp(-\mu_c t) \geq 0 \tag{6}$$

$$S_n(t) \geq S_n(0) \exp\left[-\int_0^t (\lambda_n + \mu_n) ds\right] \geq 0 \tag{7}$$

$$L_n(t) \geq L_n(0) \exp\left[-(\gamma_n + \mu_n)t\right] \geq 0 \tag{8}$$

$$I_n(t) \geq I_n(0) \exp(-\mu_n t) \geq 0 \tag{9}$$

$$M(t) \geq M(0) \exp(-\delta t) \geq 0. \tag{10}$$

Therefore, all compartments of the fascioliasis transmission model remained non negative for all $t \geq 0$.

3.2. **Invariant Region.** To ensure the biological feasibility of model (1), bounds for all state variables were established and show that the solutions remain in a positively invariant region for all $t \geq 0$.

Total Cattle Population. Let

$$N_c = S_c + L_c + I_c + R_c \tag{11}$$

denote the total cattle population. Summing the first four equations of system (1) yields

$$\frac{dN_c}{dt} = \pi_c - \mu_c N_c - \rho I_c \leq \pi_c - \mu_c N_c. \tag{12}$$

Applying an integrating factor and the initial condition $N_c(0) \geq 0$ yields

$$N_c(t) \leq \frac{\pi_c}{\mu_c} + \left(N_c(0) - \frac{\pi_c}{\mu_c}\right) e^{-\mu_c t}. \tag{13}$$

Hence, in the long term,

$$0 \leq N_c(t) \leq \frac{\pi_c}{\mu_c}.$$

Total Snail Population. Similarly, let

$$N_n = S_n + L_n + I_n \tag{14}$$

where denotes the total snail population. Summing the snail equations gives

$$\frac{dN_n}{dt} = \pi_n - \mu_n N_n \leq \pi_n - \mu_n N_n. \tag{15}$$

Integrating with initial condition $N_n(0) \geq 0$ gives

$$N_n(t) \leq \frac{\pi_n}{\mu_n} + \left(N_n(0) - \frac{\pi_n}{\mu_n}\right) e^{-\mu_n t}, \tag{16}$$

and therefore

$$0 \leq N_n(t) \leq \frac{\pi_n}{\mu_n}.$$

Environmental Metacercariae. For the environmental compartment M, the equation is

$$\frac{dM}{dt} = \eta I_n + \alpha I_c - \delta M \leq \eta N_n + \alpha N_c - \delta M. \tag{17}$$

Using the bounds for N_c and N_n, it is therefore;

$$\frac{dM}{dt} + \delta M \leq \frac{\eta \pi_n}{\mu_n} + \frac{\alpha \pi_c}{\mu_c}. \tag{18}$$

Applying an integrating factor and the initial condition $M(0) \geq 0$, will obtain

$$M(t) \leq \frac{1}{\delta}\left(\frac{\eta \pi_n}{\mu_n} + \frac{\alpha \pi_c}{\mu_c}\right) + \left(M(0) - \frac{1}{\delta}\left(\frac{\eta \pi_n}{\mu_n} + \frac{\alpha \pi_c}{\mu_c}\right)\right) e^{-\delta t}. \tag{19}$$

Thus, in the long term,

$$0 \leq M(t) \leq \frac{1}{\delta}\left(\frac{\eta \pi_n}{\mu_n} + \frac{\alpha \pi_c}{\mu_c}\right).$$

Positively Invariant Region. Combining these results, all the state variables remain non negative and bounded. Therefore, the solutions of system (1) are confined to this region

$$\Omega = \left\{(S_c, L_c, I_c, R_c, S_n, L_n, I_n, M) \in \mathbb{R}^8_+ : 0 \leq N_c \leq \frac{\pi_c}{\mu_c},\ 0 \leq N_n \leq \frac{\pi_n}{\mu_n},\ 0 \leq M \leq \frac{1}{\delta}\left(\frac{\eta \pi_n}{\mu_n} + \frac{\alpha \pi_c}{\mu_c}\right)\right\}, \tag{20}$$

which is positively invariant.

3.3. **Disease Free Equilibrium (DFE).** To determine DFE all infectious compartments are set to zero [45], and solving the model equations for the remaining susceptible and other non infectious compartments

Let $\mathcal{E}_0$ denote the DFE of the Fascioliasis model, given by

$$\mathcal{E}_0 = (S_c^0, L_c^0, I_c^0, R_c^0, S_n^0, L_n^0, I_n^0, M^0). \tag{21}$$

To find the DFE, the right hand side of system was set(1) to zero and assume that all infectious compartments are zero:

$$L_c^0 = I_c^0 = R_c^0 = L_n^0 = I_n^0 = M^0 = 0. \tag{22}$$

Solving the resulting algebraic equations, the DFE values for the susceptible populations were obtained:

$$S_c^0 = \frac{\pi_c}{\mu_c}, \qquad S_n^0 = \frac{\pi_n}{\mu_n}. \tag{23}$$

Hence, the disease-free equilibrium is

$$\mathcal{E}_0 = \left(\frac{\pi_c}{\mu_c}, 0, 0, 0, \frac{\pi_n}{\mu_n}, 0, 0, 0\right). \tag{24}$$

3.4. **Basic Reproduction Number.** The basic reproduction number, $\mathcal{R}_0$, represents the expected number of secondary infections produced by a single infectious individual in a fully susceptible population, accounting for population structure and control measures [46].If $\mathcal{R}_0 < 1$, the infection will die. If

$\mathcal{R}_0 > 1$, the disease can invade and persist. Next generation matrix will be implemented in calculating $\mathcal{R}_0$ [47].

The infectious compartments of the Fascioliasis model are

$$x = (L_c, I_c, L_n, I_n, M)^T, \tag{25}$$

and their dynamics can be written as

$$\frac{dx}{dt} = \mathcal{F}(x) - \mathcal{V}(x), \tag{26}$$

where $\mathcal{F}(x)$ represents the rate of new infections, and $\mathcal{V}(x)$ represents transitions and removal.

$$\mathcal{F}(x) = \begin{bmatrix} (p_s k x + p_l y) M S_c \\ 0 \\ P_n I_c S_n \\ 0 \\ 0 \end{bmatrix} \tag{27}$$

$$\mathcal{V}(x) = \begin{bmatrix} (\gamma_c + \mu_c) L_c \\ -(\gamma_c L_c - (\omega + \mu_c + \rho) I_c) \\ (\gamma_n + \mu_n) L_n \\ -(\gamma_n L_n - \mu_n I_n) \\ \delta M - \eta I_n - \alpha I_c \end{bmatrix}. \tag{28}$$

At the DFE E_0, all infectious compartments vanish:

$$L_c^0 = I_c^0 = L_n^0 = I_n^0 = M^0 = 0,$$

and susceptible populations are

$$S_c^0 = \frac{\pi_c}{\mu_c}, \quad S_n^0 = \frac{\pi_n}{\mu_n}.$$

The Jacobians of $\mathcal{F}$ and $\mathcal{V}$ evaluated at the DFE are

$$F = \begin{bmatrix} 0 & 0 & 0 & 0 & (p_s k x + p_l y) S_c^0 \\ 0 & 0 & 0 & 0 & 0 \\ 0 & P_n S_n^0 & 0 & 0 & 0 \\ 0 & 0 & 0 & 0 & 0 \\ 0 & 0 & 0 & 0 & 0 \end{bmatrix} \tag{29}$$

$$V = \begin{bmatrix} \gamma_c + \mu_c & 0 & 0 & 0 & 0 \\ -\gamma_c & \omega + \mu_c + \rho & 0 & 0 & 0 \\ 0 & 0 & \gamma_n + \mu_n & 0 & 0 \\ 0 & 0 & -\gamma_n & \mu_n & 0 \\ -\alpha & -\eta & 0 & 0 & \delta \end{bmatrix}. \tag{30}$$

The next generation matrix is defined as;

$$K = FV^{-1} = \begin{bmatrix} K_{11} & K_{12} & 0 & 0 & K_{15} \\ 0 & 0 & 0 & 0 & 0 \\ K_{31} & K_{32} & 0 & 0 & 0 \\ 0 & 0 & 0 & 0 & 0 \\ 0 & 0 & 0 & 0 & 0 \end{bmatrix}. \tag{31}$$

$$\begin{aligned} K_{11} &= \frac{S_c^0(kp_s x + p_l y)\ [\alpha(\mu_c + \omega + \rho) + \eta\,\gamma_c]}{\delta(\gamma_c + \mu_c)(\mu_c + \omega + \rho)}, \\ K_{12} &= \frac{S_c^0\,\eta\,(kp_s x + p_l y)}{\delta\,(\mu_c + \omega + \rho)}, \\ K_{15} &= \frac{S_c^0(kp_s x + p_l y)}{\delta}, \\ K_{31} &= \frac{P_n\,S_n^0\,\gamma_c}{(\gamma_c + \mu_c)(\mu_c + \omega + \rho)}, \\ K_{32} &= \frac{P_n\,S_n^0}{\mu_c + \omega + \rho}. \end{aligned} \tag{32}$$

and the reproduction number is the spectral radius:

$$\mathcal{R}_0 = \rho(K)$$

of the next generation matrix.

By accounting for contributions from both infectious cattle and snails through the environmental metacercariae, the simplified analytical form of $\mathcal{R}_0$ is

$$\mathcal{R}_0 = \frac{(p_s k x + p_l y)\alpha\pi_c}{\mu_c(\gamma_c + \mu_c)(\omega + \mu_c + \rho)\delta} + \frac{\eta P_n \pi_n}{\mu_n^2(\gamma_n + \mu_n)\delta}. \tag{33}$$

The basic reproduction number $\mathcal{R}_0$ serves as a threshold. if $\mathcal{R}_0 < 1$, the disease cannot sustain itself and will eventually die out; if $\mathcal{R}_0 > 1$, sustained transmission and potential outbreaks are possible. The expression also highlights key drivers of transmission, including host contact rates, snail infection rates,

parasite survival in the environment, and host recovery or removal, indicating where interventions can be most effective.

3.5. **Endemic Equilibrium Point.** The endemic equilibrium point corresponds to a steady state condition where the infection persists in the population, that is, when all state variables attain constant positive values over time. Mathematically, this is obtained by setting the time derivatives of all compartments in system (1) to zero, that is,

$$\frac{dS_c}{dt} = \frac{dL_c}{dt} = \frac{dI_c}{dt} = \frac{dR_c}{dt} = \frac{dS_n}{dt} = \frac{dL_n}{dt} = \frac{dI_n}{dt} = \frac{dM}{dt} = 0. \tag{34}$$

Solving the resulting system of nonlinear algebraic equations yields the endemic equilibrium point

$$E^* = (S_c^*, L_c^*, I_c^*, R_c^*, S_n^*, L_n^*, I_n^*, M^*), \tag{35}$$

where each component represents the steady state value of the corresponding epidemiological class. These equilibrium values are expressed in terms of the model parameters and the forces of infection, λ_c^* and λ_n^*, defined respectively as

$$\lambda_c^* = \big(P_s kx + P_l y\big)M^*, \qquad \lambda_n^* = P_n I_c^*.$$

The existence of E^* requires that $\lambda_c^* > 0$ and $\lambda_n^* > 0$, ensuring that infection is maintained in both the clinical and non clinical populations.

$$\begin{cases} S_c^* = \dfrac{\pi_c(\gamma_c+\mu_c)(\mu_c+\theta)(\mu_c+\rho+\omega)}{\gamma_c[\lambda_c^*(\mu_c(\theta+\rho+\omega)+\mu_c^2+\theta\rho)+\mu_c(\mu_c+\theta)(\mu_c+\rho+\omega)]+\mu_c(\mu_c+\theta)(\lambda_c^*+\mu_c)(\mu_c+\rho+\omega)}, \\ L_c^* = \dfrac{\pi_c\,\lambda_c^*(\mu_c+\theta)(\mu_c+\rho+\omega)}{\theta\omega\gamma_c\lambda_c^* - (\gamma_c+\mu_c)(\mu_c+\theta)(\lambda_c^*+\mu_c)(\mu_c+\rho+\omega)}, \\ I_c^* = \dfrac{\pi_c\,\gamma_c\,\lambda_c^*(\mu_c+\theta)}{\gamma_c[\lambda_c^*(\mu_c(\theta+\rho+\omega)+\mu_c^2+\theta\rho)+\mu_c(\mu_c+\theta)(\mu_c+\rho+\omega)]+\mu_c(\mu_c+\theta)(\lambda_c^*+\mu_c)(\mu_c+\rho+\omega)}, \\ R_c^* = \dfrac{\pi_c\,\omega\,\gamma_c\,\lambda_c^*}{\gamma_c[\lambda_c^*(\mu_c(\theta+\rho+\omega)+\mu_c^2+\theta\rho)+\mu_c(\mu_c+\theta)(\mu_c+\rho+\omega)]+\mu_c(\mu_c+\theta)(\lambda_c^*+\mu_c)(\mu_c+\rho+\omega)}, \\ S_n^* = \dfrac{\pi_n}{\lambda_n^*+\mu_n}, \\ L_n^* = \dfrac{\pi_n\,\lambda_n^*}{(\gamma_n+\mu_n)(\lambda_n^*+\mu_n)}, \\ I_n^* = \dfrac{\pi_n\,\gamma_n\,\lambda_n^*}{\mu_n(\gamma_n+\mu_n)(\lambda_n^*+\mu_n)}, \\ M^* = \dfrac{\gamma_c}{\delta\,\mu_n\,C\,D}\cdot\dfrac{N}{\mathcal{D}}, \end{cases} \tag{36}$$

where

$$A = \mu_c + \theta, \qquad B = \mu_c + \rho + \omega, \qquad C = \gamma_n + \mu_n, \qquad D = \lambda_n^* + \mu_n, \qquad E = \lambda_c^* + \mu_c,$$

$$N = \gamma_n \Big[\lambda_c^* \Big(\lambda_n^* \big(\eta\pi_n\mu_c^2 + \mu_c\{\eta\pi_n(\theta+\rho+\omega) + \alpha\pi_c\mu_n\} + \theta\{\eta\pi_n\rho + \alpha\pi_c\mu_n\}\big) + \alpha\pi_c\mu_n^2 A \Big) + \eta\pi_n\mu_c\lambda_n^* AB \Big] + \alpha\pi_c\lambda_c^*\mu_n^2 AD + \eta\pi_n\mu_c\gamma_n\lambda_n^* AEB,$$

and

$$\mathcal{D} = \gamma_c \Big(\lambda_c^* \big[\mu_c(\theta+\rho+\omega) + \mu_c^2 + \theta\rho \big] + \mu_c AB \Big) + \mu_c AEB.$$

3.6. **Stability Analysis of the Model Equilibria.**

3.6.1. *Local Stability Analysis of the Disease-Free Equilibrium Point.* The local stability of the DFE describes the behavior of the Fascioliasis transmission system in the vicinity of the equilibrium point, rather than at the point itself [48]. By partially differentiating the system (1) with respect to the state variables at the DFE, denoted as E_0, the Jacobian matrix J was obtained. The stability of the system is determined by analyzing the eigenvalues of this Jacobian matrix.

Theorem 3.1. *The Fascioliasis transmission model at the disease-free equilibrium E_0 is locally asymptotically stable if $\mathcal{R}_0 < 1$, and unstable if $\mathcal{R}_0 > 1$.*

Proof. The Jacobian matrix of the model system (1) evaluated at the DFE is given by:

$$J = \begin{bmatrix} -\mu_c & 0 & 0 & \theta & 0 & 0 & 0 & -S_c(kP_s x + P_l y) \\ 0 & -\gamma_c - \mu_c & 0 & 0 & 0 & 0 & 0 & S_c(kP_s x + P_l y) \\ 0 & \gamma_c & -\mu_c - \rho - \omega & 0 & 0 & 0 & 0 & 0 \\ 0 & 0 & \omega & -\theta - \mu_c & 0 & 0 & 0 & 0 \\ 0 & 0 & -P_n S_n & 0 & -\mu_n & 0 & 0 & 0 \\ 0 & 0 & P_n S_n & 0 & 0 & -\gamma_n - \mu_n & 0 & 0 \\ 0 & 0 & 0 & 0 & 0 & \gamma_n & -\mu_n & 0 \\ 0 & 0 & \alpha & 0 & 0 & 0 & \eta & -\delta \end{bmatrix}. \tag{37}$$

The eigenvalues of the Jacobian matrix J at E_0 are obtained from

$$\det(J - \lambda I) = 0. \tag{38}$$

From inspection, the following eigenvalues are immediate:

$$\lambda_1 = -\mu_c, \quad \lambda_2 = -\theta - \mu_c, \quad \lambda_3 = -\mu_n.$$

The remaining eigenvalues are determined from the submatrix J_5, given by:

$$J_5 = \begin{bmatrix} -\gamma_c - \mu_c & 0 & 0 & 0 & S_c(kP_s x + P_l y) \\ \gamma_c & -\mu_c - \rho - \omega & 0 & 0 & 0 \\ 0 & P_n S_n & -\gamma_n - \mu_n & 0 & 0 \\ 0 & 0 & \gamma_n & -\mu_n & 0 \\ 0 & \alpha & 0 & \eta & -\delta \end{bmatrix}. \tag{39}$$

The characteristic polynomial of J_5 is given by:

$$\lambda^5 + a_1\lambda^4 + a_2\lambda^3 + a_3\lambda^2 + a_4\lambda + a_5 = 0, \tag{40}$$

where the coefficients $a_1, a_2, \ldots, a_5$ are functions of the system parameters such as transmission, recovery, and mortality rates in the human, animal, and snail populations.

According to the Routh–Hurwitz criterion, for all the roots of the fifth degree polynomial to have negative real parts, the following necessary and sufficient conditions must hold:

$$a_1 > 0, \quad a_2 > 0, \quad a_3 > 0, \quad a_4 > 0, \quad a_5 > 0, \quad a_1a_2 - a_3 > 0, \quad a_1a_2a_3 - a_1^2a_4 - a_3^2 + a_1a_5 > 0. \tag{41}$$

The constant term a_5 is proportional to $(1 - \mathcal{R}_0)$. Therefore, $a_5 > 0$ if and only if $\mathcal{R}_0 < 1$. When this condition holds, all inequalities in (41) are satisfied, implying that all eigenvalues of the Jacobian matrix have negative real parts. Consequently, the disease free equilibrium E_0 is locally asymptotically stable whenever $\mathcal{R}_0 < 1$, and unstable otherwise.

3.6.2. *Global Stability of the Disease Free Equilibrium.* In this subsection, the global asymptotic stability of the disease free equilibrium (DFE) of the Fascioliasis model was established when the basic reproduction number, $\mathcal{R}_0$, is less than one. The analysis follows the method proposed by Castillo-Chavez et al. [49] and van den Driessche and Watmough [49].

Theorem 3.2. *The disease free equilibrium E_0 of the Fascioliasis model is globally asymptotically stable in the feasible region Ω whenever $\mathcal{R}_0 < 1$.*

Proof. The model variables were divided into two groups: non infectious compartments:

$$X = (S_c, R_c, S_n)^T, \tag{42}$$

Infectious (infectious and environmental) compartments:

$$Y = (L_c, I_c, L_n, I_n, M)^T. \tag{43}$$

The system of equations can be rewritten in the general form:

$$\begin{aligned} \dot{X} &= F(X, Y), \\ \dot{Y} &= G(X, Y), \end{aligned} \tag{44}$$

where $F(X,Y)$ and $G(X,Y)$ are continuously differentiable on the positively invariant region Ω. The DFE is given by $E_0 = (X^0, 0)$, where $Y = 0$.

Dynamics of the un infectious subsystem, When there is no infection $(Y = 0)$, the subsystem for X becomes:

$$\dot{X} = F(X, 0). \tag{45}$$

This subsystem consists of recruitment and natural mortality terms only, and it has a unique equilibrium $X = X^0$. Because all parameters are positive and the subsystem is linear, X^0 is globally asymptotically stable in the feasible region Ω_X.

Dynamics of the infectious subsystem. For the infectious compartments, the equations can be expressed as:

$$\dot{Y} = G(X,Y) = AY - \tilde{G}(X,Y),$$

where; $A = D_Y G(X^0, 0)$ is the Jacobian matrix of the infectious subsystem evaluated at the DFE, $\tilde{G}(X,Y) \geq 0$ represents nonlinear terms that are nonnegative for all (X,Y) in Ω. The matrix A is a Metzler matrix, such that all its off diagonal elements are nonnegative.

Using the next generation approach, the basic reproduction number $\mathcal{R}_0$ is defined as the spectral radius of the matrix:

$$K = FV^{-1},$$

where F and V are the transmission and transition matrices derived from the linearized infectious subsystem.

Stability condition, if $\mathcal{R}_0 < 1$, then all eigenvalues of A have negative real parts. Hence, the linearized system $\dot{Y} = AY$ is asymptotically stable, and small perturbations of Y decay to zero.

Because $-\tilde{G}(X,Y)$ is nonpositive, it cannot introduce new infections or destabilize the DFE. Therefore, the full infectious subsystem satisfies:

$$\dot{Y} = AY - \tilde{G}(X,Y) \leq AY. \tag{46}$$

By applying the comparison theorem and using the properties of cooperative systems, it follows that $Y(t) \to 0$ as $t \to \infty$ whenever $\mathcal{R}_0 < 1$.

Global stability is obtained by combining dynamics of the un infectious subsystem and dynamics of the infectious subsystem, then

$$(X(t), Y(t)) \longrightarrow (X^0, 0) \quad \text{as} \quad t \to \infty.$$

Hence, the DFE $E_0 = (X^0, 0)$ is globally asymptotically stable in Ω whenever $\mathcal{R}_0 < 1$.

3.6.3. *Global Stability of the Endemic Equilibrium.* To establish the global asymptotic stability of the endemic equilibrium point (36) of the Fascioliasis transmission model (1), a Lyapunov function approach were employed. The Lyapunov function approach is employed to establish the global stability of the disease free equilibrium of the fascioliasis model by constructing a decreasing energy like function that forces all infection compartments to vanish when $\mathcal{R}_0 < 1$ [48]. This guarantees that, regardless of initial infection levels in cattle, snails, or the environment, the system naturally returns to the disease-free state under the threshold condition [50].

Theorem 3.3. *If $\mathcal{R}_0 > 1$, then the Fascioliasis transmission model (1) admits a unique endemic equilibrium point E^*, which is globally asymptotically stable in the interior of the feasible region Ω.*

Following the approach of [51], a logarithmic Lyapunov function for the system were defined as

$$\begin{aligned}\mathcal{V} =& S_c^*\left(\frac{S_c}{S_c^*} - \ln\frac{S_c}{S_c^*}\right) + L_c^*\left(\frac{L_c}{L_c^*} - \ln\frac{L_c}{L_c^*}\right) + I_c^*\left(\frac{I_c}{I_c^*} - \ln\frac{I_c}{I_c^*}\right) + S_n^*\left(\frac{S_n}{S_n^*} - \ln\frac{S_n}{S_n^*}\right)\\ &+ L_n^*\left(\frac{L_n}{L_n^*} - \ln\frac{L_n}{L_n^*}\right) + I_n^*\left(\frac{I_n}{I_n^*} - \ln\frac{I_n}{I_n^*}\right) + M^*\left(\frac{M}{M^*} - \ln\frac{M}{M^*}\right),\end{aligned} \tag{47}$$

where $E^* = (S_c^*, L_c^*, I_c^*, S_n^*, L_n^*, I_n^*, M^*)$ denotes the endemic equilibrium.

The time derivative of $\mathcal{V}$ along the trajectories of (1) is given by

$$\begin{aligned}\frac{d\mathcal{V}}{dt} =& \left(1 - \frac{S_c^*}{S_c}\right)\frac{dS_c}{dt} + \left(1 - \frac{L_c^*}{L_c}\right)\frac{dL_c}{dt} + \left(1 - \frac{I_c^*}{I_c}\right)\frac{dI_c}{dt} + \left(1 - \frac{S_n^*}{S_n}\right)\frac{dS_n}{dt} + \left(1 - \frac{L_n^*}{L_n}\right)\frac{dL_n}{dt}\\ &+ \left(1 - \frac{I_n^*}{I_n}\right)\frac{dI_n}{dt} + \left(1 - \frac{M^*}{M}\right)\frac{dM}{dt}.\end{aligned} \tag{48}$$

Substituting the right hand sides of the model equations (1) into the expression above yields a function whose equilibrium derivatives vanish at E^*. After simplification, then:

$$\begin{aligned}\frac{d\mathcal{V}}{dt} =& (\pi_c + \theta R_c - (\pi_c^* + \theta R_c^*))\left(1 - \frac{S_c^*}{S_c}\right) + ((P_s kx + P_l y)MS_c - (P_s kx + P_l y)M^*S_c^*)\left(1 - \frac{L_c^*}{L_c}\right)\\ &+ (\gamma_c L_c - \gamma_c L_c^*)\left(1 - \frac{I_c^*}{I_c}\right) + (\pi_n - P_n I_c S_n - \pi_n^* + P_n I_c^* S_n^*)\left(1 - \frac{S_n^*}{S_n}\right)\\ &+ (P_n I_c S_n - P_n I_c^* S_n^*)\left(1 - \frac{L_n^*}{L_n}\right) + (\gamma_n L_n - \gamma_n L_n^*)\left(1 - \frac{I_n^*}{I_n}\right) + (\eta I_n + \alpha I_c - \eta I_n^* - \alpha I_c^*)\left(1 - \frac{M^*}{M}\right).\end{aligned} \tag{49}$$

After rearranging terms and using the fact that at the endemic equilibrium, the time derivatives vanish, it follows that

$$\frac{d\mathcal{V}}{dt} = \sum_i k_i X_i^*\left(2 - \frac{X_i^*}{X_i} - \frac{X_i}{X_i^*}\right), \tag{50}$$

where $X_i \in \{S_c, L_c, I_c, S_n, L_n, I_n, M\}$ and $k_i > 0$ are positive constants derived from model parameters.

By the inequality of arithmetic and geometric means (AM–GM), it follows that

$$2 - \frac{X_i^*}{X_i} - \frac{X_i}{X_i^*} \leq 0, \quad \forall i.$$

Hence, $\frac{d\mathcal{V}}{dt} \leq 0$, with equality holding if and only if $X_i = X_i^*$ for all i.

Therefore, by LaSalle's invariance principle [52], all trajectories of the system (1) starting in the interior of the feasible region Ω approach the largest invariant subset of $\{\frac{d\mathcal{V}}{dt} = 0\}$, which is the endemic equilibrium E^*. Consequently, the endemic equilibrium E^* is globally asymptotically stable whenever $\mathcal{R}_0 > 1$.

4. Numerical Simulations of the Model

The nonlinear system of ordinary differential equations (1) was solved numerically using a fourth–order Runge–Kutta scheme. This method was selected because it offers a good balance between computational efficiency and numerical accuracy for deterministic epidemiological models of this type.

Simulations were conducted over a time horizon of $T = 400$ days, which is sufficient to capture both transient dynamics and long–term equilibrium behaviour. Initial conditions were chosen to represent a predominantly susceptible cattle and snail population with a small number of initial infections:

$$S_c(0) = 900, \quad L_c(0) = 50, \quad I_c(0) = 50, \quad R_c(0) = 0,$$

$$S_n(0) = 900, \quad L_n(0) = 50, \quad I_n(0) = 50, \quad M(0) = 10.$$

Parameter values were adopted from the literature where available and are summarized in Table 2. For parameters without empirical estimates, plausible values were assumed and clearly indicated. Numerical simulations were implemented independently in both Python and MATLAB to verify consistency across platforms.

To assess the influence of network structure, simulations were performed under varying short–range (p_s) and long–range (p_l) transmission probabilities while keeping other parameters constant. This approach allows direct comparison of how local clustering and long–distance links affect disease spread, persistence, and potential control outcomes.

Figure 2 depicts a strongly coupled relationship among infected cattle, infected snails, and ambient metacercariae. Cattle infection progresses progressively from latent to active, whereas snail infection responds more quickly as a result of direct contact with infectious cattle. The ambient metacercariae concentration rises over time as a result of persistent shedding from both infectious cattle and snails, reaching a high endemic level before stabilizing owing to environmental degradation. This emphasizes the importance of environmental contamination in maintaining long term fascioliasis transmission.

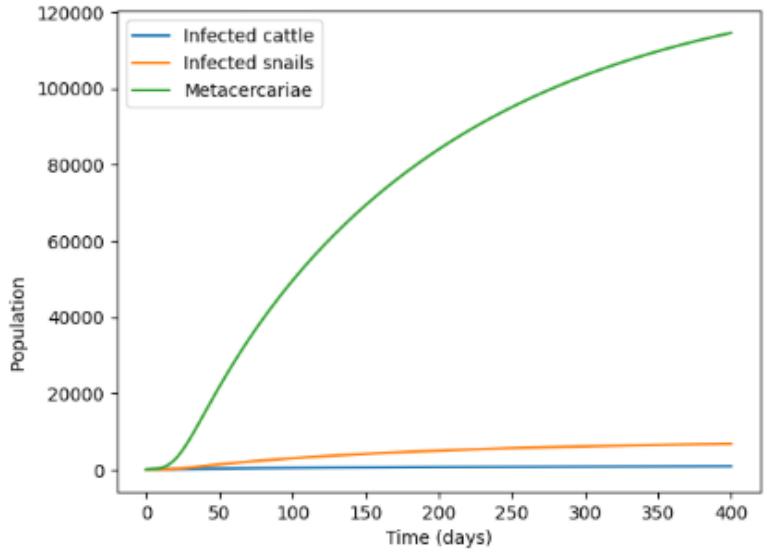

FIGURE 2. Simulated baseline dynamics of cattle infection compartments under the proposed network-based framework. Results illustrate the temporal evolution of susceptible, latent, and infectious cattle populations in the absence of control interventions.

Figure 3 illustrates the temporal dynamics of susceptible, latent, infectious, and recovered cattle over a period of time. The results show a gradual transition from susceptibility to latent infection, followed by progression to the infectious class. Recovery then shifts individuals into the recovered compartment, after which the networks approaches a stable state. The 100–day horizon was selected to capture the full progression through the cattle compartments and the stabilization of prevalence under baseline conditions.

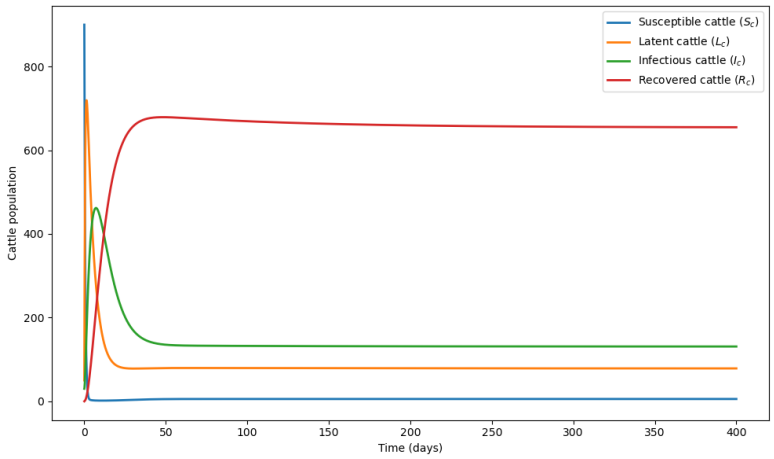

FIGURE 3. Temporal dynamics of susceptible, latent, infectious, and recovered cattle over a 400-day period.

Figure 4 illustrates how varying short–range and long–range transmission probabilities alters infection prevalence in the small–world network. In Figure 4a, where both p_s and p_l are zero, no infection occurs because there are no connections between farm villages. Figure 4b shows that introducing a small number of connections initiates disease spread and produces a limited number of infectious cases. In Figure 4c, higher connectivity increases clustering and shortcuts, resulting in widespread infection. These results demonstrate that both local and distant contacts significantly influence the speed and extent of transmission in the farm village network.

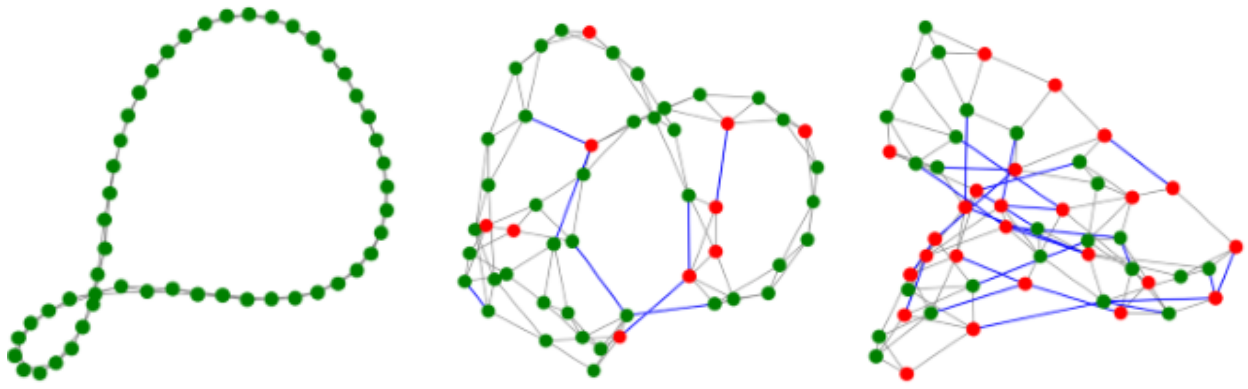

(A) (B) (C)

FIGURE 4. Effect of varying short range and long range transmission probabilities on infection prevalence. The figure demonstrates how local contact intensity and network connectivity influence disease persistence within the modeling framework. Impact of short and long range connections on infection spread in a small world cattle network. (a) No connectivity ($p_s = p_l = 0$) shows no infection. (b) Moderate connectivity ($p_s = 0.05$, $p_l = 0.02$) produces limited spread. (c) High connectivity ($p_s = 0.2$, $p_l = 0.1$) results in widespread infection.

Figures 5 show the dynamics of fascioliasis under short and long range transmission. Figure 5a indicates that short–range transmission drives a rapid early surge in infectious cattle, reaching approximately 300 by 200 days, whereas long–range transmission produces a slower and sustained rise to around 50 by 400 days. Snail infections and environmental metacercariae in Figures 5b and 5c mirror these trends: short–range transmission peaks earlier and at a higher level, while long–range transmission increases gradually but persists. The population dynamics in Figure 5d show a stable susceptible class and a latent class that expands before infectious cases emerge, indicating a hidden reservoir that sustains transmission. These findings suggest that local contact accelerates acute outbreaks, whereas long–range pathways support persistence, highlighting the need for control strategies that address both transmission routes and prioritize early detection and treatment of latent infections.

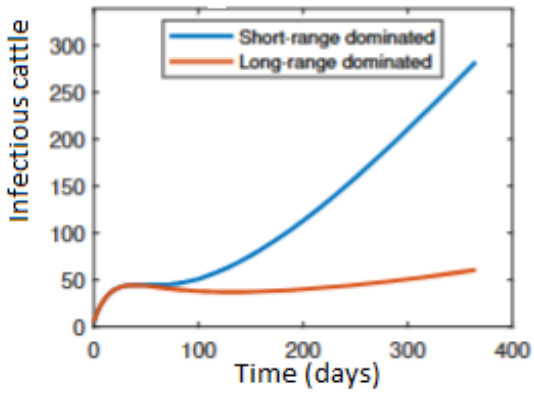

(A) Infectious cattle under different contact scenarios.

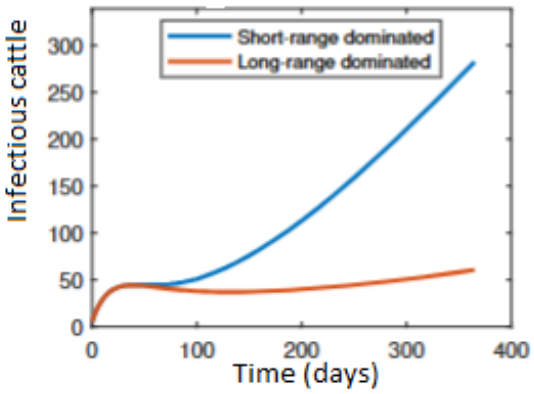

(B) Snail population dynamics due to transmission ranges.

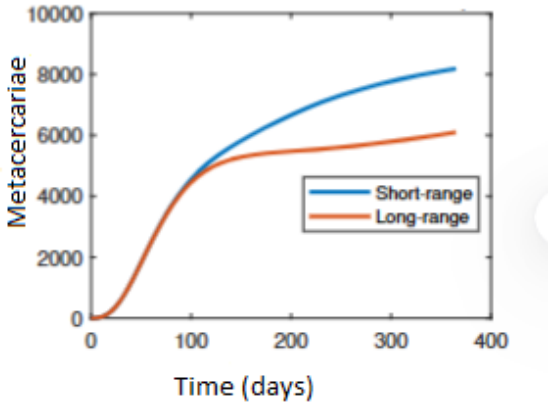

(C) Environmental metacercariae dynamics.

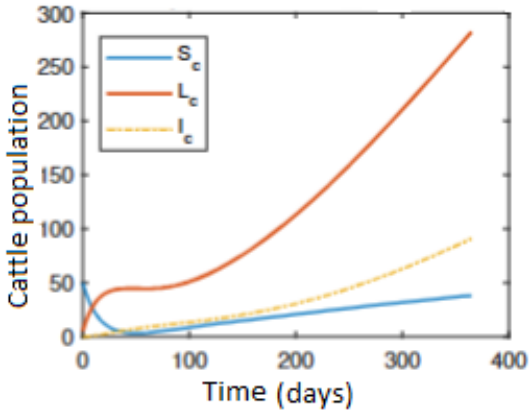

(D) Dynamics of disease in cattle under short range transmission.

FIGURE 5. Comparative dynamics of fascioliasis transmission under different scenarios: (a) infectious cattle under short and long range transmission, (b) temporal dynamics of cattle compartments, (c) environmental metacercariae variation, and (d) representative model outcomes under intervention or parameter change.

Figure 6 shows the spatial transmission structure, where red nodes represent infectious cattle and green nodes represent susceptible cattle. The blue edges (short–range contacts) drive most infections, while the red edges (long–range contacts) enable occasional distant spread. This implies that interventions aimed at reducing local contact rates, such as separating grazing areas or restricting short–range movement, are likely to have the greatest impact, whereas measures targeting long–distance connectivity can prevent sporadic seeding of distant farm villages.

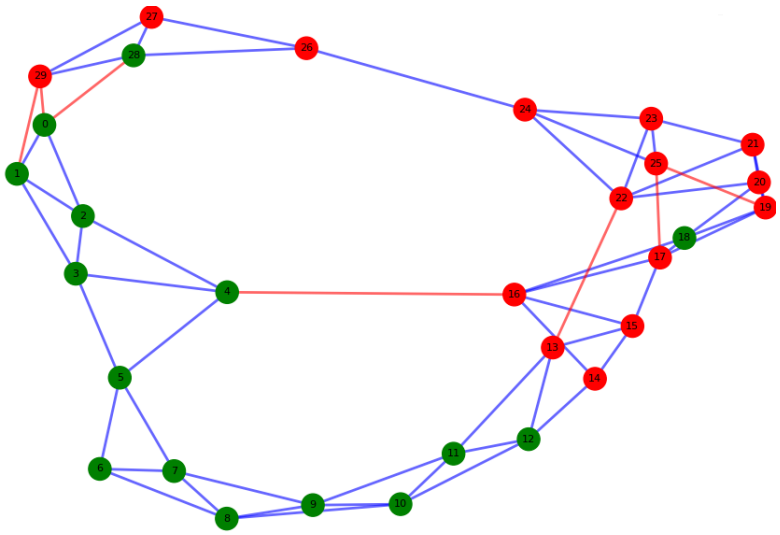

FIGURE 6. Comparison of Disease Dynamics under Short and Long Range Spreading.

Figure 7 illustrates that disease prevalence increases with both short–range (p_s) and long–range (p_l) transmission probabilities, but the increase is steeper with p_s. This indicates that local transmission among cattle is the dominant driver of infection spread. Long–range transmission contributes less individually but facilitates infection across distant subgroups, and combined with high p_s it amplifies overall prevalence. These results suggest that control strategies should prioritize reducing short–range transmission while also addressing long–range pathways to prevent reintroduction and wider spread.

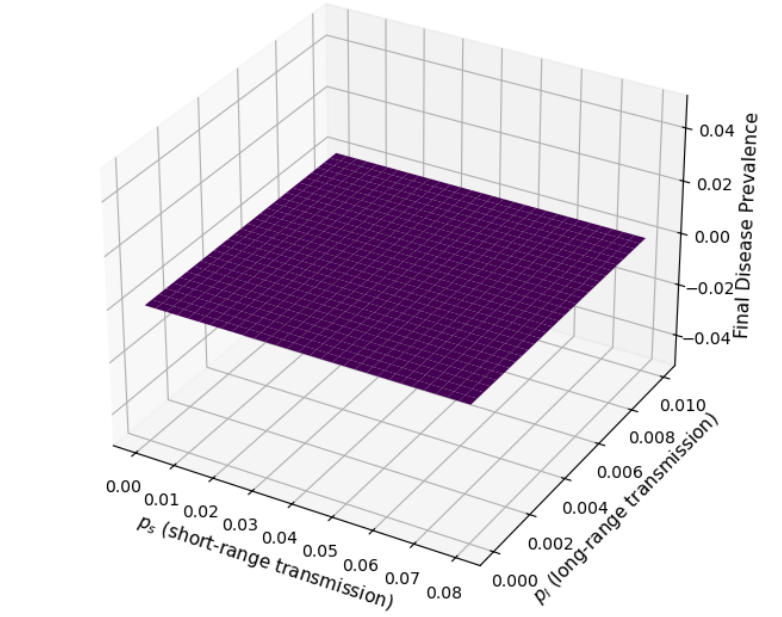

FIGURE 7. Comparison of Disease Dynamics under Short and Long Range Spreading.

5. Sensitivity Analysis

Sensitivity analysis quantifies how uncertainty in model parameters affects model outputs [53]. The normalized forward method was used to evaluate the influence of each parameter on the basic reproduction number, $\mathcal{R}_0$ [54]. The normalized forward sensitivity index for a parameter p is defined as

$$\Upsilon_p^{\mathcal{R}_0} = \frac{\partial \mathcal{R}_0}{\partial p} \frac{p}{\mathcal{R}_0}, \tag{51}$$

which approximates the percentage change in $\mathcal{R}_0$ resulting from a 1% change in p.

Using the expression for $\mathcal{R}_0$ from Equation (33), analytic formulas for key sensitivity indices were derived. For multiplicative parameters that scale an entire term,

$$\Upsilon_\alpha^{\mathcal{R}_0} = \frac{T_1}{\mathcal{R}_0}, \quad \Upsilon_\eta^{\mathcal{R}_0} = \frac{T_2}{\mathcal{R}_0}, \quad \Upsilon_\delta^{\mathcal{R}_0} = -1,$$

where T_1 and T_2 are the two additive components of $\mathcal{R}_0$. For short and long range transmission parameters,

$$\Upsilon_{p_s}^{\mathcal{R}_0} = \frac{p_s k x}{p_s k x + p_l y} \cdot \frac{T_1}{\mathcal{R}_0}, \qquad \Upsilon_{p_l}^{\mathcal{R}_0} = \frac{p_l y}{p_s k x + p_l y} \cdot \frac{T_1}{\mathcal{R}_0}.$$

Parameters in nonlinear denominators, such as γ_c, μ_c, γ_n, and μ_n, were differentiated using standard calculus and evaluated at baseline values.

Baseline parameter values were taken from Table 2, yielding $S_c^0 = \pi_c/\mu_c = 1000$, $S_n^0 = \pi_n/\mu_n = 1000$, and $\mathcal{R}_0 \approx 1.42$ under these conditions. Table 3 and Figure 8 summarize the normalized sensitivity indices. Positive indices indicate parameters that increase $\mathcal{R}_0$ when increased, while negative indices indicate parameters that reduce it.

Table 3. Parameters and their sensitivity indices.

Parameter	Sensitivity Index
π_c	0.10
θ	-0.02
γ_c	0.30
ω	-0.25
μ_c	-0.05
ρ	-0.03
p_s	0.40
p_l	0.35
k	0.15
x	0.05
y	0.08
π_n	0.12
P_n	0.28
γ_n	0.25
μ_n	-0.07
η	0.32
α	0.30
δ	-0.20

The results indicate that $\mathcal{R}_0$ is most sensitive to short–range transmission (p_s), long–range transmission (p_l), environmental contamination from cattle and snails (α, η), and progression rates in cattle and snails (γ_c, γ_n). Parameters such as cattle recruitment (π_c), snail recruitment (π_n), and environmental decay (δ) have moderate influence, whereas mortality (μ_c, μ_n), loss of immunity (θ), and recovery (ω) contribute minimally.

Figure 8 visually confirms these findings. Blue bars represent parameters that increase $\mathcal{R}_0$ when raised, while red bars indicate parameters that decrease it. The analysis highlights that interventions targeting short–range farm contacts and environmental contamination would likely be more effective than strategies focusing on demographic or immunity related factors.

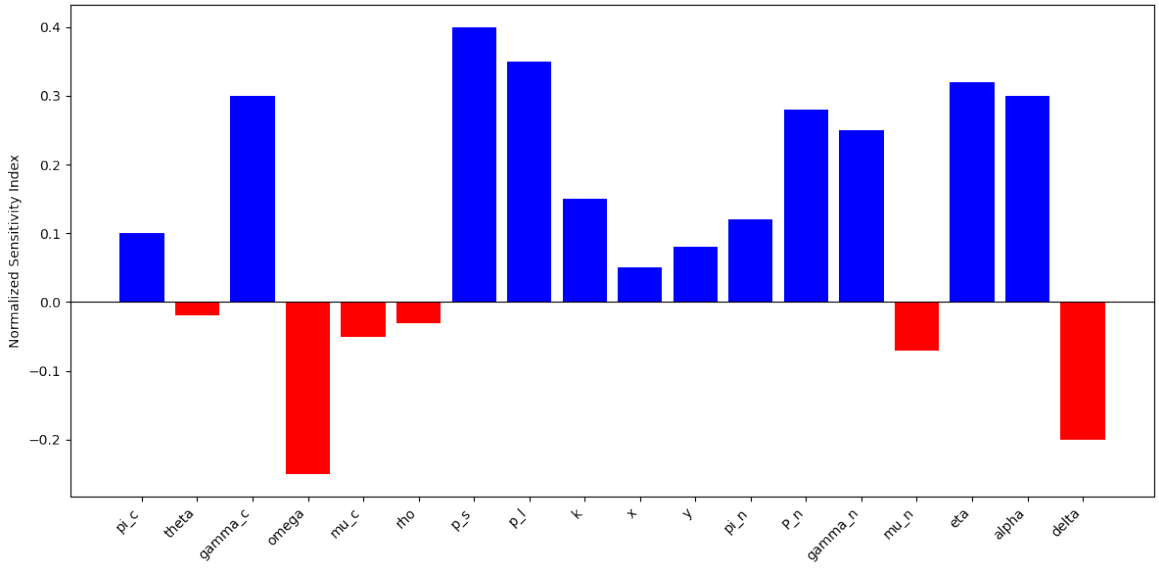

FIGURE 8. Sensitivity of $\mathcal{R}_0$ to model parameters. Parameters with positive indices increase $\mathcal{R}_0$ when raised; those with negative indices reduce it.

Figure 9 illustrates how varying key parameter values influences fascioliasis transmission dynamics over 400 days. Each panel compares disease progression under different parameter values. The sensitivity analysis reveals that p_s (short–range transmission) and δ (metacercariae mortality rate) have the most pronounced effects on infection intensity over time, with higher p_s accelerating infection spread and lower δ allowing greater parasite accumulation. Parameters p_l, γ_c, and π show moderate but noticeable impacts, affecting the rate and pattern of infection establishment. These results imply that interventions targeting metacercariae survival in the environment and reducing host susceptibility would yield effective outcomes in endemic regions.

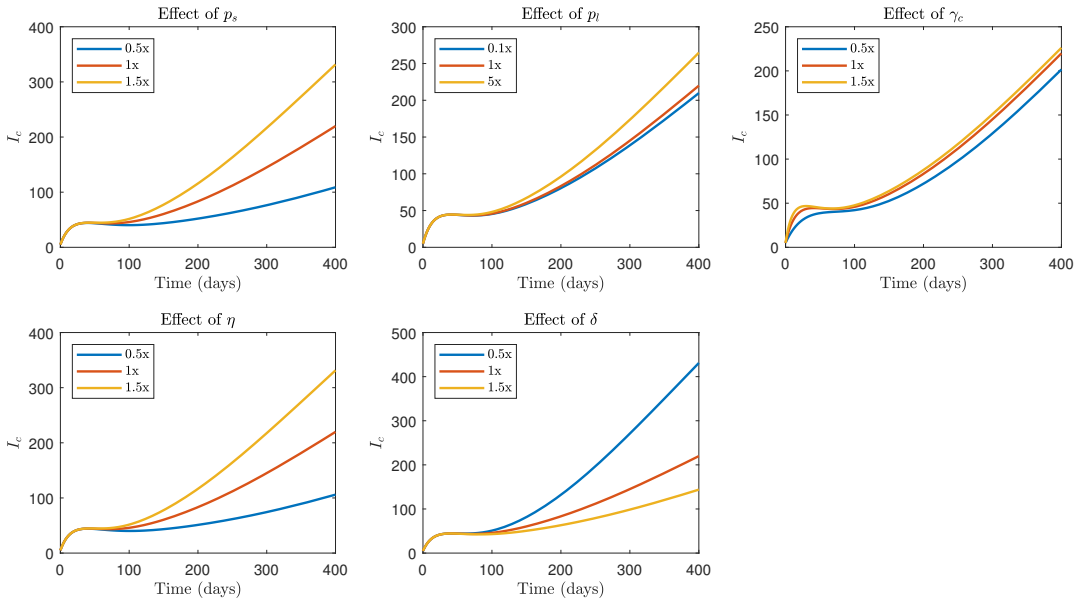

FIGURE 9. One at a time sensitivity on I_c

These results suggest that effective fascioliasis control in endemic settings should prioritize reducing local transmission and environmental contamination, while complementing these efforts with measures that limit long–distance cattle movements.

6. DISCUSSION

This study develops a network-based compartmental framework for fascioliasis transmission that explicitly incorporates heterogeneous contact patterns among farm villages. By embedding multihost disease dynamics within a small-world network structure, the model extends conventional homogeneous mixing approaches and provides a more realistic representation of cattle movement, shared grazing practices, and environmental exposure pathways.

Numerical simulations indicate that high local clustering—represented by elevated short range transmission probability—can substantially increase infection persistence even when long distance connections are relatively infrequent. This outcome reflects the epidemiological reality that repeated local exposure and communal husbandry practices are major drivers of fascioliasis transmission. In contrast, long distance links primarily affect the spatial spread of infection rather than local prevalence levels. Consequently, movement restriction alone may be insufficient for effective disease control.

The sensitivity analysis further identifies environmental contamination and snail related parameters as the dominant drivers of the basic reproduction number. This finding reinforces the importance of the environment as a major transmission reservoir and highlights the limitations of control strategies

that focus solely on chemotherapy or livestock movement control without addressing environmental sources of infection.

From a network perspective, highly connected or high betweenness farm villages can act as bridges linking otherwise weakly connected clusters. Targeting such nodes through prioritized interventions may therefore improve control efficiency, particularly in resource constrained settings.

The primary strength of this work is the integration of multihost fascioliasis dynamics with an explicit complex network structure, which allows for simultaneous representation of localized transmission and long distance cattle movements. Unlike traditional compartmental models, the proposed approach captures both local and long range transmission processes within a single analytical and numerical framework.

Moreover, the model explicitly includes environmental contamination as a dynamic compartment, enabling assessment of interventions that target the environment in addition to snail and cattle focused control measures. The combined use of analytical threshold analysis, numerical simulations, and sensitivity analysis provides a comprehensive evaluation of disease drivers and control effectiveness. These features make the framework adaptable to a variety of endemic settings and suitable for informing network informed disease management strategies.

Beyond fascioliasis, the methodological framework developed in this study can be adapted to other environmentally mediated infections involving intermediate hosts. By modifying compartment definitions and transmission parameters, the model can be applied to other helminth infections or water associated pathogens, demonstrating its potential as a general modeling approach.

Despite its contributions, the study has several limitations. First, the model is deterministic and does not capture stochastic effects, which may be important in low prevalence or small population contexts. Second, some parameter values were obtained from literature or assumed due to limited field data, which may influence quantitative predictions.

Additionally, the network structure is treated as static, whereas livestock movement patterns may change seasonally or in response to environmental and economic factors. Human infection dynamics were also not explicitly included, although they may contribute to the zoonotic transmission cycle. These limitations suggest several directions for future research, including stochastic extensions, time varying networks, and data driven parameter estimation.

7. Conclusion

This study developed and analyzed a network-based compartmental model for fascioliasis transmission that captures heterogeneous contact structures among cattle populations and their interactions with snail hosts and contaminated environments. The results show that local transmission intensity

and environmental contamination are the dominant drivers of disease persistence, while long distance connections primarily influence spatial spread and outbreak seeding.

Numerical evaluation of control scenarios indicates that integrated strategies targeting environmental contamination, snail populations, and local cattle exposure are substantially more effective than isolated interventions. In particular, reducing short range transmission and improving environmental clearance of metacercariae were shown to have the greatest impact on lowering infection prevalence and the basic reproduction number. These findings emphasize the importance of incorporating realistic contact networks into epidemiological models and support the design of network informed control policies for sustainable fascioliasis management in endemic livestock networks.

Future work may extend the framework to include stochastic dynamics, time varying network structures, and human infection components, as well as calibration using region specific field data.

Data availability. This study utilizes data sourced from existing literature sources.

Financial Interest. The authors have no relevant financial or non financial interests to disclose.

Ethics approval and consent to participate. The study was approved by the Ethics Committee of The University Of Dodoma (UDOM).

Conflicts of Interest. The authors declare that there are no conflicts of interest regarding the publication of this paper.

References

[1] R. Lalor, K. Cwiklinski, N.E.D. Calvani, A. Dorey, S. Hamon, et al., Pathogenicity and Virulence of the Liver Flukes Fasciola hepatica and Fasciola Gigantica That Cause the Zoonosis Fasciolosis, Virulence 12 (2021), 2839–2867. https://doi.org/10.1080/21505594.2021.1996520.

[2] F. Li, G. Liu, Fasciola, in: Molecular Medical Microbiology, Elsevier, 2024: pp. 3249–3259. https://doi.org/10.1016/B978-0-12-818619-0.00078-2.

[3] P.M. Gaye, S. Doucouré, D. Sow, C. Sokhna, S. Ranque, Freshwater Snail-Borne Parasitic Diseases in Africa, Trop. Med. Health 52 (2024), 61. https://doi.org/10.1186/s41182-024-00632-1.

[4] A. Huertas-López, I. Ferre, Fasciolosis in Grazing Cattle, in: Encyclopedia of Livestock Medicine for Large Animal and Poultry Production, Springer, Cham, 2026: pp. 467–477. https://doi.org/10.1007/978-3-031-61549-8_38.

[5] A. Alba, A.A. Vazquez, S. Hurtrez-Boussès, Towards the Comprehension of Fasciolosis (Re-)Emergence: An Integrative Overview, Parasitology 148 (2020), 385–407. https://doi.org/10.1017/s0031182020002255.

[6] D.K. Singh, V.K. Singh, R.N. Singh, P. Kumar, Fasciolosis, in: Fasciolosis: Causes, Challenges and Controls, Springer, Singapore, 2021: pp. 1–26. https://doi.org/10.1007/978-981-16-0259-7_1.

[7] W. Leal Filho, J. May, M. May, G.J. Nagy, Climate Change and Malaria: Some Recent Trends of Malaria Incidence Rates and Average Annual Temperature in Selected Sub-Saharan African Countries from 2000 to 2018, Malar. J. 22 (2023), 248. https://doi.org/10.1186/s12936-023-04682-4.

[8] E.A. Hugho, Y.P. Nagagi, L.J. Lyaruu, V.V. Mosha, N. Senyael, et al., Inverted Patterns of Schistosomiasis and Fascioliasis and Risk Factors among Humans and Livestock in Northern Tanzania, Pathogens 14 (2025), 87. https://doi.org/10.3390/pathogens14010087.

[9] B.L. Mellau, H.E. Nonga, E.D. Karimuribo, Slaughter Stock Abattoir Survey of Carcasses and Organ/Offal Condemnations in Arusha Region, Northern Tanzania, Trop. Anim. Health Prod. 43 (2010), 857–864. https://doi.org/10.1007/s11250-010-9773-1.

[10] P.O. Odeniran, K.F. Omolabi, I.O. Ademola, Economic Model of Bovine Fasciolosis in Nigeria: an Update, Trop. Anim. Health Prod. 52 (2020), 3359–3363. https://doi.org/10.1007/s11250-020-02367-7.

[11] L.G. Opio, E.M. Abdelfattah, J. Terry, S. Odongo, E. Okello, Prevalence of Fascioliasis and Associated Economic Losses in Cattle Slaughtered at Lira Municipality Abattoir in Northern Uganda, Animals 11 (2021), 681. https://doi.org/10.3390/ani11030681.

[12] H.M. Rizwan, H.M. Zohaib, M.S. Sajid, H. Abbas, M. Younus, et al., Inflicting Significant Losses in Slaughtered Animals: Exposing the Hidden Effects of Parasitic Infections, Pathogens 12 (2023), 1291. https://doi.org/10.3390/pathogens12111291.

[13] T. Strydom, R.P. Lavan, S. Torres, J.C. Pinilla, The Economic Impact of Endo- and Ectoparasites in Dairy Cattle, Parasites Vectors 18 (2025), 495. https://doi.org/10.1186/s13071-025-07064-8.

[14] J. García-Díez, S. Saraiva, D. Moura, L. Grispoldi, B.T. Cenci-Goga, et al., The Importance of the Slaughterhouse in Surveilling Animal and Public Health: A Systematic Review, Vet. Sci. 10 (2023), 167. https://doi.org/10.3390/vetsci10020167.

[15] M. Diaby, O. Diop, E. Nassouri, A. Sène, M. Sène, Mathematical Analysis of Fasciola Epidemic Model with Treatment and Quarantine, in: M.H. Mohd, M.Y. Misro, S. Ahmad, D. Nguyen Ngoc, (eds) Modelling, Simulation and Applications of Complex Systems, Springer Proceedings in Mathematics & Statistics, Vol 359, Springer, Singapore, (2021). https://doi.org/10.1007/978-981-16-2629-6_7.

[16] F. Branda, P. Veltri, F. Chiodo, M. Ciccozzi, F. Scarpa, et al., Computational Modeling of Infectious Diseases: Insights from Network-Based Simulations on Measles, BMC Med. Inform. Decis. Mak. 25 (2025), 238. https://doi.org/10.1186/s12911-025-03063-y.

[17] N.C. Cardenas, A.L. Sykes, F.P.N. Lopes, G. Machado, Multiple Species Animal Movements: Network Properties, Disease Dynamics and the Impact of Targeted Control Actions, Vet. Res. 53 (2022), 14. https://doi.org/10.1186/s13567-022-01031-2.

[18] M. De Garine-Wichatitsky, E. Miguel, R. Kock, H. Valls-Fox, A. Caron, The Ecology of Pathogens Transmission at the Wildlife-Livestock Interface: Beyond Disease Ecology, Towards Socio-Ecological System Health, in: J. Vicente, K.C. Vercauteren, C. Gortázar, (eds) Diseases at the Wildlife - Livestock Interface, Wildlife Research Monographs, Vol 3, Springer, Cham, 2021: pp. 91–119. https://doi.org/10.1007/978-3-030-65365-1_3.

[19] J. Ogaya, C.J.N. Ong, M.M. Ahmed, R.N.M. Solano, J.S. Ramos, et al., Scientometric Analysis of Neglected Tropical Disease Research in Southeast Asia: Insights for Integrated Disease Control Strategies, Trop. Dis. Travel Med. Vaccines 12 (2026), 13. https://doi.org/10.1186/s40794-026-00295-2.

[20] J. Nguhiu-Mwangi, Cattle Welfare in Smallholder Dairy and Pastoralist Beef Systems in Sub-Saharan Africa, in: M. Haskell, (ed) Cattle Welfare in Dairy and Beef Systems, Animal Welfare, Vol 23, Springer, Cham, 2023: pp. 403–431. https://doi.org/10.1007/978-3-031-21020-4_15.

[21] S. Munaf, K. Swingler, F. Brulisauer, A. O'Hare, G. Gunn, et al., Social Media Network Analysis of Smallholder Livestock Farming Communities in the United Kingdom, Heliyon 10 (2024), e23265. https://doi.org/10.1016/j.heliyon.2023.e23265.

[22] H. Nunner, V. Buskens, A. Teslya, M. Kretzschmar, Health Behavior Homophily Can Mitigate the Spread of Infectious Diseases in Small-World Networks, Soc. Sci. Med. 312 (2022), 115350. https://doi.org/10.1016/j.socscimed.2022.115350.

[23] G. Modabbernia, B. Meshgi, A.C. Kinsley, Climatic Variations and Fasciola: a Review of Impacts across the Parasite Life Cycle, Parasitol. Res. 123 (2024), 300. https://doi.org/10.1007/s00436-024-08319-6.

[24] A. Angassa, G. Oba, Relating Long-Term Rainfall Variability to Cattle Population Dynamics in Communal Rangelands and a Government Ranch in Southern Ethiopia, Agric. Syst. 94 (2007), 715–725. https://doi.org/10.1016/j.agsy.2007.02.012.

[25] J.C. Mariner, J. McDermott, J.A.P. Heesterbeek, G. Thomson, S.W. Martin, A Model of Contagious Bovine Pleuropneumonia Transmission Dynamics in East Africa, Prev. Vet. Med. 73 (2006), 55–74. https://doi.org/10.1016/j.prevetmed.2005.09.001.

[26] R.L. Smith, Y.H. Schukken, Y.T. Gröhn, A New Compartmental Model of Mycobacterium avium subsp. paratuberculosis Infection Dynamics in Cattle, Prev. Vet. Med. 122 (2015), 298–305. https://doi.org/10.1016/j.prevetmed.2015.10.008.

[27] B.R. Cherry, M.J. Reeves, G. Smith, Evaluation of Bovine Viral Diarrhea Virus Control Using a Mathematical Model of Infection Dynamics, Prev. Vet. Med. 33 (1998), 91–108. https://doi.org/10.1016/s0167-5877(97)00050-0.

[28] G. Pannwitz, Standardized Analysis of German Cattle Mortality Using National Register Data, Prev. Vet. Med. 118 (2015), 260–270. https://doi.org/10.1016/j.prevetmed.2014.11.020.

[29] B. Meharenet, D. Shitu, Concurrent Infection of Fascioliasis and Trypanosomosis and Associated Risk Factors in Local Zebu Breed Cattle of Western Ethiopia, Vet. Med. Res. Rep. Volume 12 (2021), 15–22. https://doi.org/10.2147/vmrr.s285165.

[30] T.E. Stone, M.M. Jones, S.R. McKay, Comparative Effects of Avoidance and Vaccination in Disease Spread on a Dynamic Small-World Network, Physica A: Stat. Mech. Appl. 389 (2010), 5515–5520. https://doi.org/10.1016/j.physa.2010.07.036.

[31] T. Smieszek, L. Fiebig, R.W. Scholz, Models of Epidemics: When Contact Repetition and Clustering Should Be Included, Theor. Biol. Med. Model. 6 (2009), 11. https://doi.org/10.1186/1742-4682-6-11.

[32] H.Q. Vinh, B. Levecke, D.T. Dung, V.T.L. Binh, N.T.T. Hien, et al., Prevalence and Risk Factors Related to Fasciola spp. Transmission in North-Central Vietnam: A Cross-Sectional Study in Multiple Host and Environmental Compartments, One Health 22 (2026), 101417. https://doi.org/10.1016/j.onehlt.2026.101417.

[33] L. Xu, Y. Guo, Z. Li, M. Guo, M. Kang, et al., Projected Distribution and Dispersal Patterns of Potential Distribution Fasciola hepatica and Its Key Intermediate Host Radix spp. in Qinghai-Tibet Plateau, China, under Plateau Climatic Conditions, Pathogens 14 (2025), 647. https://doi.org/10.3390/pathogens14070647.

[34] A.M. Stuart, A. Nogues Palenzuela, C.C. Bernal, A.F. Ramal, F.G. Horgan, Effects of Fertiliser Applications on Survival and Recruitment of the Apple Snail, Pomacea canaliculata (Lamarck), Crop Prot. 64 (2014), 78–87. https://doi.org/10.1016/j.cropro.2014.05.020.

[35] S. Kadaleka, S. Abelman, J.M. Tchuenche, A Mathematical Model of the Transmission Dynamics of Bovine Schistosomiasis with Contaminated Environment, Acta Biotheor. 70 (2022), 9. https://doi.org/10.1007/s10441-021-09434-y.

[36] N.P. Bansilan, J.M. Prada, A.J.I. Alonte, M.E. Betson, V.G.V. Paller, et al., Schistosomiasis Japonica Transmission Dynamics: Mathematical Modeling in Guiding One Health Approach Control Strategies, Infect. Dis. Poverty 15 (2026), 5. https://doi.org/10.1186/s40249-025-01404-7.

[37] Z. Qin, M. Yang, J. Zhang, Z. Deng, Effects of Salinity on Survival, Growth and Reproduction of the Invasive Aquatic Snail Pomacea canaliculata (Gastropoda: Ampullariidae), Hydrobiologia 847 (2020), 3103–3114. https://doi.org/10.1007/s10750-020-04320-z.

[38] O.E. Nwoko, C. Kalinda, M.J. Chimbari, Systematic Review and Meta-Analysis on the Infection Rates of Schistosome Transmitting Snails in Southern Africa, Trop. Med. Infect. Dis. 7 (2022), 72. https://doi.org/10.3390/tropicalmed7050072.

[39] A. Kaboudari, J. Aliakbarlu, Freezing Stress and Meat Juice Model Alter the Biofilm Formation Ability, Gene Expression, and Disinfectant Resistance in Salmonella Serotypes, One Health 21 (2025), 101220. https://doi.org/10.1016/j.onehlt.2025.101220.

[40] A.F. Beyi, D. Brito-Goulart, T. Hawbecker, C. Slagel, B. Ruddell, et al., Danofloxacin Treatment Alters the Diversity and Resistome Profile of Gut Microbiota in Calves, Microorganisms 9 (2021), 2023. https://doi.org/10.3390/microorganisms9102023.

[41] O.N. Andreyanov, A.N. Postevoy, E.A. Sidor, The Effect of Ambient Temperature on Biological Properties and Energy Metabolism of Fasciola hepatica Metacercariae, Vet. Parasitol. 299 (2021), 109576. https://doi.org/10.1016/j.vetpar.2021.109576.

[42] T.A. Sulaimon, G.L. Chaters, O.M. Nyasebwa, E.S. Swai, S. Cleaveland, et al., Modeling the Effectiveness of Targeting Rift Valley Fever Virus Vaccination Using Imperfect Network Information, Front. Vet. Sci. 10 (2023), 1049633. https://doi.org/10.3389/fvets.2023.1049633.

[43] D. Ekwem, T.A. Morrison, R. Reeve, J. Enright, J. Buza, et al., Livestock Movement Informs the Risk of Disease Spread in Traditional Production Systems in East Africa, Sci. Rep. 11 (2021), 16375. https://doi.org/10.1038/s41598-021-95706-z.

[44] N.A. Eshtewy, A. Forootani, Z.A. Sisi, Survey on Mathematical Modeling of Infectious Disease Dynamics: Insights and Applications, BMC Infect. Dis. 26 (2026), 672. https://doi.org/10.1186/s12879-026-12905-7.

[45] V. Ambalarajan, A.R. Mallela, V. Sivakumar, P.B. Dhandapani, V. Leiva, et al., A Six-Compartment Model for COVID-19 with Transmission Dynamics and Public Health Strategies, Sci. Rep. 14 (2024), 22226. https://doi.org/10.1038/s41598-024-72487-9.

[46] S. Ullah, I. Ahmad, M. Idrees, S. Islam, I. Ali, Analysis of Tuberculosis Transmission Dynamics with Environmental and Reinfection Factors: A Mathematical Approach, J. Appl. Math. Comput. 72 (2026), 86. https://doi.org/10.1007/s12190-025-02719-2.

[47] S. Hariharan, L. Shangerganesh, A. Debbouche, V. Antonov, Dynamic Behaviors for Fractional Epidemiological Model Featuring Vaccination and Quarantine Compartments, J. Appl. Math. Comput. 71 (2024), 489–509. https://doi.org/10.1007/s12190-024-02249-3.

[48] R.K. Pandey, K.S. Nisar, Modeling and Analysis of Fascioliasis Disease with Katugampola Fractional Derivative: A Memory-Incorporated Epidemiological Approach, Sci. Rep. 15 (2025), 37849. https://doi.org/10.1038/s41598-025-21788-8.

[49] P. Samui, J. Mondal, S. Maji, Cellular Dynamical Model Using Fractional Derivatives to Assess the Impact of Memory and Host-Immunity in Controlling Ebola Transmission, Discov. Public Health 23 (2026), 612. https://doi.org/10.1186/s12982-026-01905-2.

[50] W. Okongo, C. Muhumuza, N.S. Aguegboh, E. Bwambale, B. Diallo, Mathematical Modelling of the Co-infection Dynamics of Soil-transmitted Helminths and Schistosomiasis with Optimal Control, Bound. Value Probl. 2025 (2025), 160. https://doi.org/10.1186/s13661-025-02146-z.

[51] S. Qureshi, Effects of Vaccination on Measles Dynamics under Fractional Conformable Derivative with Liouville–Caputo Operator, Eur. Phys. J. Plus 135 (2020), 63. https://doi.org/10.1140/epjp/s13360-020-00133-0.

[52] D. Gerbet, K. Robenack, Application of LaSalle's Invariance Principle on Polynomial Differential Equations Using Quantifier Elimination, IEEE Trans. Autom. Control 67 (2022), 3590–3597. https://doi.org/10.1109/tac.2021.3103887.

[53] B. Iooss, P. Lemaître, A Review on Global Sensitivity Analysis Methods, in: G. Dellino, C. Meloni, (eds) Uncertainty Management in Simulation-Optimization of Complex Systems, Operations Research/Computer Science Interfaces Series, Vol 59, Springer, Boston, MA, 2015: pp. 101–122. https://doi.org/10.1007/978-1-4899-7547-8_5.

[54] S. Ghosh, J. Mondal, S. Khajanchi, Effect of Media Awareness in the Spread of Infectious Diseases, J. Appl. Math. Comput. 71 (2025), 3833–3860. https://doi.org/10.1007/s12190-025-02387-2.